SKBF
KBS
TEKNISK RAPPORT
80-16

Permeability of highly compacted bentonite

Roland Pusch

Division Soil Mechanics, University of Luleå 1980-12-23

SVENSK KÄRNBRÄNSLEFÖRSÖRJNING AB / PROJEKT KÄRNBRÄNSLESÄKERHET

POSTADRESS: Kärnbränslesäkerhet, Box 5864, 102 48 Stockholm, Telefon 08-67 95 40

PERMEABILITY OF HIGHLY COMPACTED BENTONITE

Roland Pusch

Division Soil Mechanics, University of Luleå
1980-12-23

A list of other reports published in this series is attached at the end of this report. Information on KBS technical reports from 1977-1978 (TR 121) and 1979 (TR 79-28) is available through SKBF/KBS.

PERMEABILITY OF HIGHLY COMPACTED BENTONITE

KBS PROJ. 15:06

BY ROLAND PUSCH

LULEÅ 1980-12-23

DIV. SOIL MECHANICS, UNIVERSITY OF LULEÅ

CONTENTS

INTRODUCTION

The clay barrier of the KBS concept concerning the storage of unreprocessed nuclear fuel wastes, consists of highly compacted bentonite. It is applied in the form of blocks so as to fill the space between the metal canisters and the surrounding rock. Since the bentonite is not fully saturated at its deposition, it takes up additional water from the rock and ultimately becomes saturated. This migration, which has the character of unsaturated flow, has been discussed previously (PUSCH, 1980).

When the saturation is completed, and when normal temperatures finally prevail, water flow through the bentonite is caused by hydraulic gradients which will be very small shortly after the final sealing of the repository. Despite the resulting low rate of flow in this phase the water percolation is still of great importance because of the very long periods of time that have to be considered. This matter is the object of the present study which comprised laboratory tests and theoretical considerations concerning the permeability of water-saturated bentonite.

EXPERIMENTAL

Equipment and techniques

In this study water flow was considered on a macroscopic scale, and the permeability was evaluated by applying the DARCY equation:

$$\frac{q}{A} = k \cdot i \qquad (1)$$

where q = flow per time unit (measured quantity)
A = cross section area (known property)
k = coefficient of permeability
i = hydraulic gradient (evaluated from measured pressure and sample height)

The way of measuring the rate of water flow under a constant gradient is a straightforward and simple technique which, however, involves some wellknown practical difficulties, such as the risk of leakage or non-uniform percolation. The only alternative method would be to calculate the permeability by fitting TERZAGHI's theory of consolidation (TERZAGHI, 1923) to observed laboratory time/settlement observations and extracting the coefficient of permeability from the calculated coefficient of consolidation. This would require fairly low bulk densities, however, and a disadvantage would also be that the hydraulic gradient cannot be kept constant, neither at high nor at low values.

The first-mentioned technique was applied in this study, the experimental determination of the flow rate being made by means of the LuH swelling pressure oedometer (Fig. 1).

Each test involved compaction of "air-dry" bentonite to the desired density, and a subsequent water uptake under confined conditions. At the end of the water saturation period, the duration of which being related to the height of the sample, the lower filter stone was connected to a cylindrical vessel in which de-aired water was compressed by using a piston operated by means of high air pressure. This device has been frequently used for producing back pressures in triaxial tests of various soils and is known to transfer the pressure to the liquid with practically no loss through friction or leakage (Fig. 2). This was confirmed in the present study by continuously recording the water pressure (transducer technique).

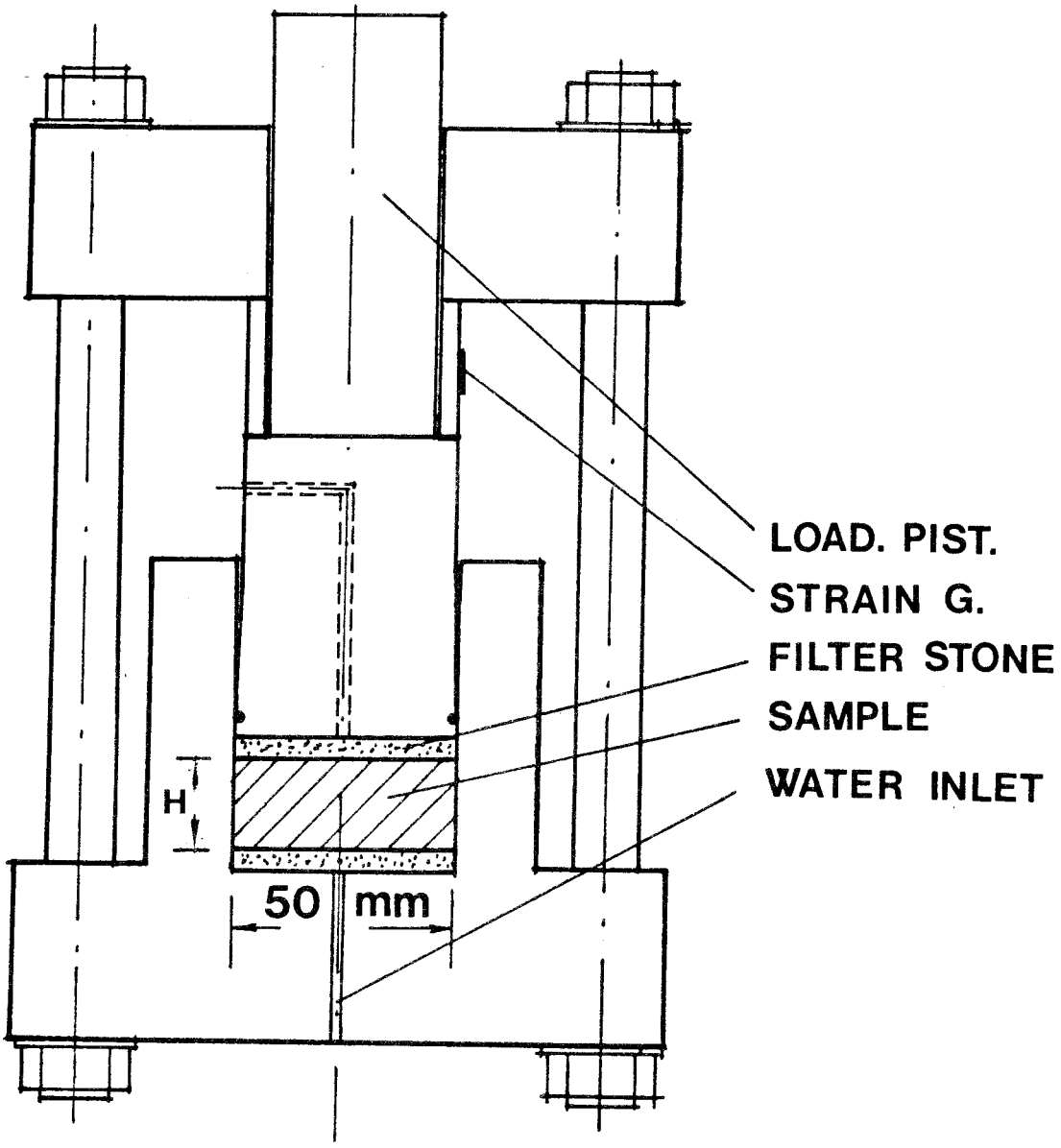

Fig. 1. The LuH swelling pressure oedometer. The compacted sample was confined between the filter stones through which water passed during the period of saturation as well as in the percolation test. The "loading piston" was used only to determine the swelling pressure.

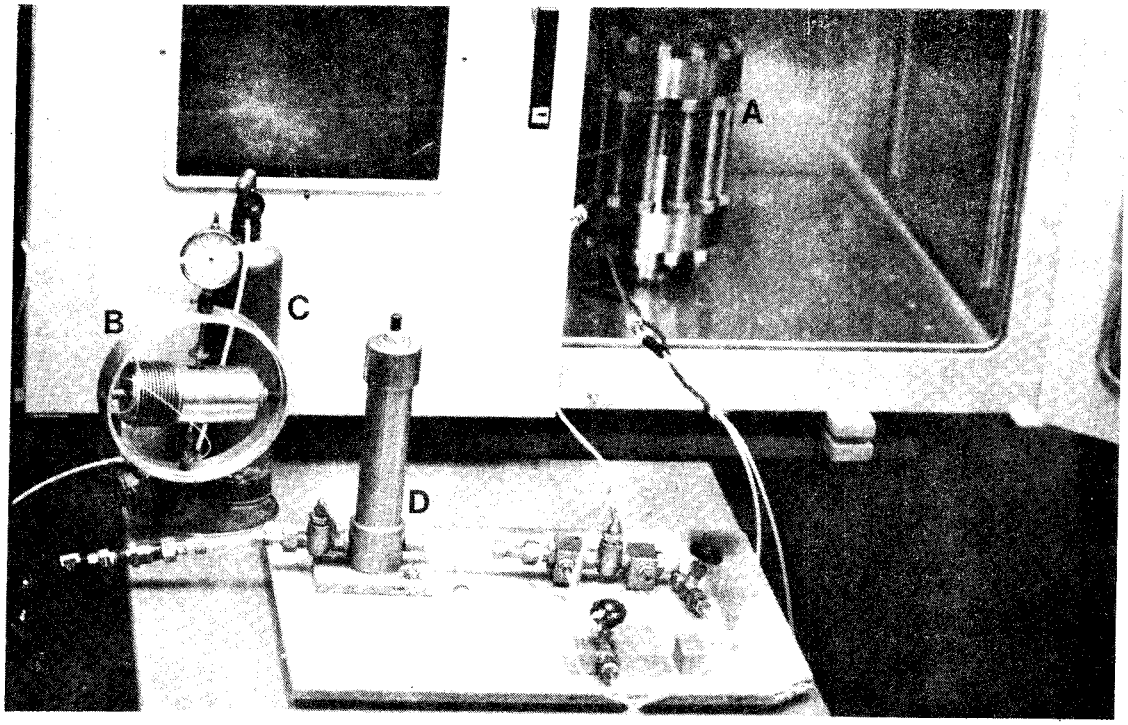

A = Oedometer
B = Cylinder with piston
C = Gas container
D = Pipe with transducer

Fig. 2. Experimental set-up for the permeability tests.

The compacted samples were approximately 5 mm thick. Separate investigations of the rate of water uptake (PUSCH, 1980), show that such thin samples become completely water saturated after approximately 1 day, but the percolation experiments were not started until 3 days after the beginning of the water uptake to guarantee that all voids were water-filled prior to the percolation.

In most tests the pressure was varied systematically in the order 500 kPa, 250 kPa, 100 kPa, and 50 kPa to find out whether the hydraulic gradient affects the permeability or not. Each resulting gradient, referring to 5 mm sample height, (10^4, $5 \cdot 10^3$, $2 \cdot 10^3$ and 10^3, respectively) was kept constant until stationary flow conditions were obtained or approached. The total testing time required for each sample was therefore rather long, 3-4 weeks as an average. Separate tests were run at 20°C and 70°C, the bulk density being within the interval 1.87 to 2.21 t/m^3. In these tests the oedometer was kept in an oven, the temperature of which could be maintained at 70°C with great accuracy.

The percolated water quantities were extremely small as a consequence of the very low permeability, and the flow rate could therefore not be determined with sufficient accuracy by applying sampling and weighing techniques. Instead, it was directly determined by observing the rate of displacement of a water meniscus in a calibrated capillary connected to the filter stone at the water exit. The accuracy of the evaluated permeability was estimated at approximately $5 \cdot 10^{-15}$ m/s. The technique is similar to the one used by HANSBO (1960). The common problem of leakage along the confining walls when performing percolation tests on soft clays is largely eliminated when testing dense bentonites, since their high swelling pressure produces a tight contact with the walls.

Clay materials and water

Granulometry and mineralogy

Two commercially available bentonites were used for the production of samples of highly compacted clay; the American

Colloid Co. type MX-80 (Na Wyoming bentonite) being the main KBS reference material, and the Erbslöh Ca bentonite, representing a natural calcium-saturated clay material.

Both bentonites are characterized by a minus 2 µm content of approximately 85%, and a montmorillonite content of about 80-90% of this fraction. Silt is the dominant remaining fraction which mainly contains quartz and feldspars as well as some micas, sulphides and oxides.

The two bentonites are not purely sodium- or calcium-saturated clay materials. Thus, spectrometric analyses have shown that the Erbslöh Ca bentonite contains 20-60 mg Ca, 15-30 mg Mg, and 20-40 mg Na per liter of pore water. This relatively small difference points to fairly similar physical properties and current investigations of the swelling pressure also confirm that the two bentonites behave similarly at high bulk densities. The permeability should be much more influenced by the pore water chemistry, however, since it has a strong impact on the degree of aggregation. This was also verified by the experiments.

Water

The KBS reference water, "Allard's" solution (cf. KBS Report 98) which is a synthetic ground water (91 mg of cations and 215 mg of anions per liter), was used for water saturation and percolation in all the tests. It is considered to be representative of the ground water at 500 m depth in Swedish crystalline rock.

Microstructure, clay/water interaction

The influence of microstructural features on water uptake and migration processes in bentonites has been discussed previously by author (PUSCH, 1980). Since they are fundamental also of the understanding and proper evaluation of the flow records, the matter is dealt with in some detail in the present report as well.

In principle, the microstructure of granulated, "air-dry" bentonite powders, compacted at their natural water contents (approximately 10%), can be illustrated by Fig. 3.

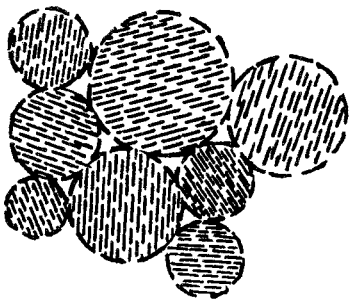

Fig. 3. Schematic microstructure of compacted "air-dry" MX-80.

The aggregates consist of small fragments of the natural bentonite clay beds and since the Wyoming deposits are heavily preconsolidated and structurally anisotropic (cf. Fig. 4), the fragments are also anisotropic and consist of flaky particles which are largely parallel. The aggregates are characterized by a very small interparticle and interlamellar spacing in the original "air-dry" condition of the MX-80 powder. Similar conditions are valid for the Erbslöh bentonite as well, although the air-dry powder is more fine-grained than the MX-80 product.

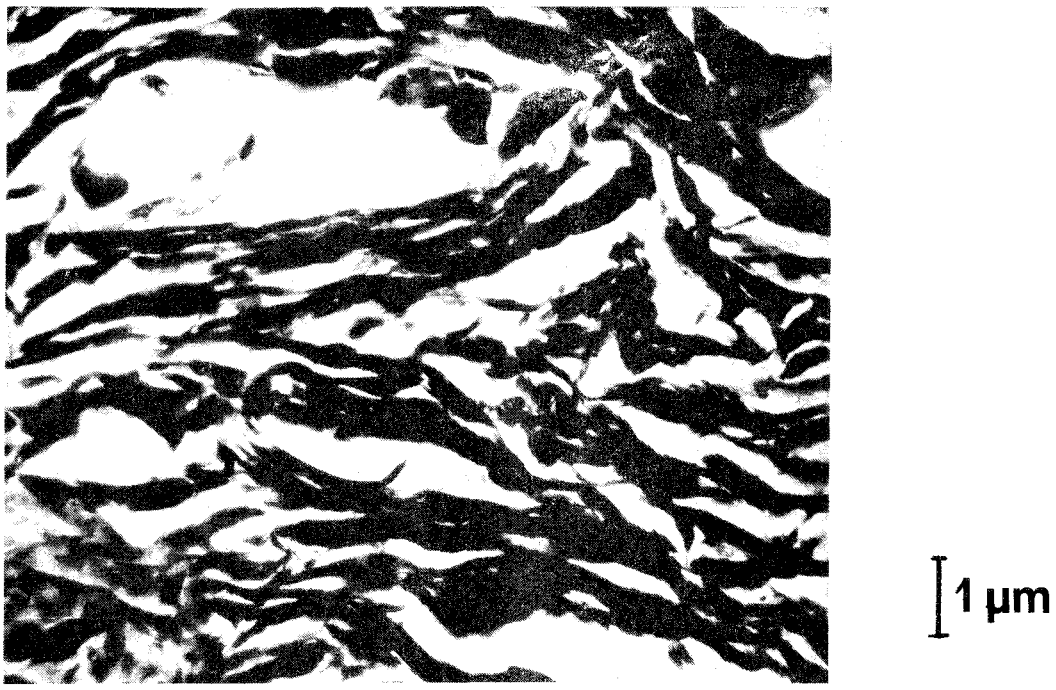

Fig. 4. Electron micrograph of montmorillonitic clay (London clay) preconsolidated under 300 m sediment. Notice the high degree of preferred orientation.

When the granulated bentonite powders are compressed to form blocks of "highly compacted bentonite", the aggregates are forced together. At moderate pressures and uniaxial compression, as well as at isotropic compression under any pressure, the overall particle orientation is largely random, while uniaxial compression under very high pressures yields a tendency of the particles to be oriented perpendicularly to the applied pressure. Even very high pressures cannot produce a homogeneous structural pattern and the microstructure will consequently consist of aggregates and voids in between,regardless of the applied compaction pressure. Naturally, however, the voids will be smaller and the aggregates more deformed at high pressures.

In the course of the water saturation the aggregates expand and, if given sufficient time, most of the larger interparticle voids will be filled by a clay gel formed by the expanding aggregates. Eventually, a condition of considerable isotropy and homogeneity with respect to particle orientation and interparticle distance will be reached at moderate and high densities in Na bentonite. The average particle spacing, without reference to inter- or intraparticle (interlamellar) distances, is schematically illustrated by Fig. 5.

The larger swelling ability of Na bentonite than of Ca bentonite suggests that many voids in the latter clay will not be completely gel-filled when the aggregates expand in course of the saturation. A higher permeability of Ca bentonite is therefore expected, although the difference between the two clay types should not be very large.

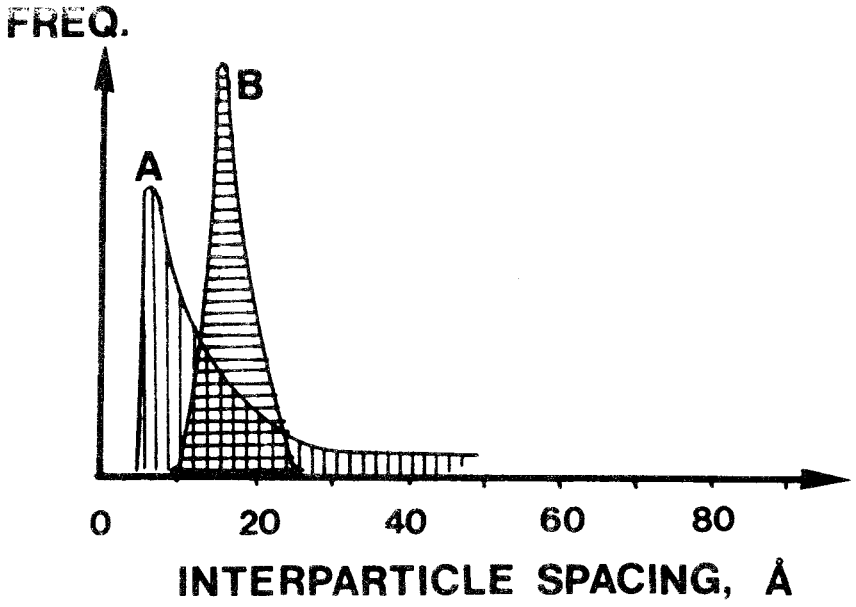

Fig. 5. Schematic distributions of the interparticle spacing. A) original spectrum for "air-dry" bentonite. B) narrow peak for homogeneous, swollen sample with high density.

Test program

While the air-dry bentonite powders had an initial water content of approximately 10% in all the tests, the saturated samples were given largely varying bulk densities and water contents in order to investigate the relationship between these properties and the permeability. The test program is shown in Table 1.

Table 1. Test program

Test No.	Material	Bulk density ρ_m, t/m^3	Water content[1] %	Compaction pressure MPa	Temperature °C
1	MX-80	1.90	46	3.0	20
2	MX-80	1.95	46	3.3	20
3	MX-80	1.97	39	5.0	20
4	MX-80	2.15	27	27.5	20
5	MX-80	1.93	38	9.0	70
6	MX-80	1.95	45	1.6	70
7	MX-80	2.10	27	29.0	70
8	Erbslöh	1.94	39	5.1	20
9	Erbslöh	2.21	30	30.2	20
10	Erbslöh	1.87	44	4.7	70
11	Erbslöh	1.93	37	10.0	70
12	Erbslöh	2.13	29	29.0	70

1) Determined after the end of each test

Test results

The evaluated permeability was found to be a function of the hydraulic gradient as illustrated by the example in Fig. 6 and 7. The deviation from DARCY's law is rather moderate but the trend is obvious as shown by Table 2, especially for the MX-80. Although the general trend was that of Fig. 6, meaning that the evaluated permeability was successively reduced following each gradient reduction, the flow was not steady. Daily variations of as much as ±5 to 10% of the ultimate value were observed, especially following gradient changes (Fig. 7). This cannot be due to an unsufficient accuracy of the experimental technique except, possibly, for Test 2; it probably has to do with certain fundamental features of gradient-induced flow in clays, as will be discussed in the subsequent text.

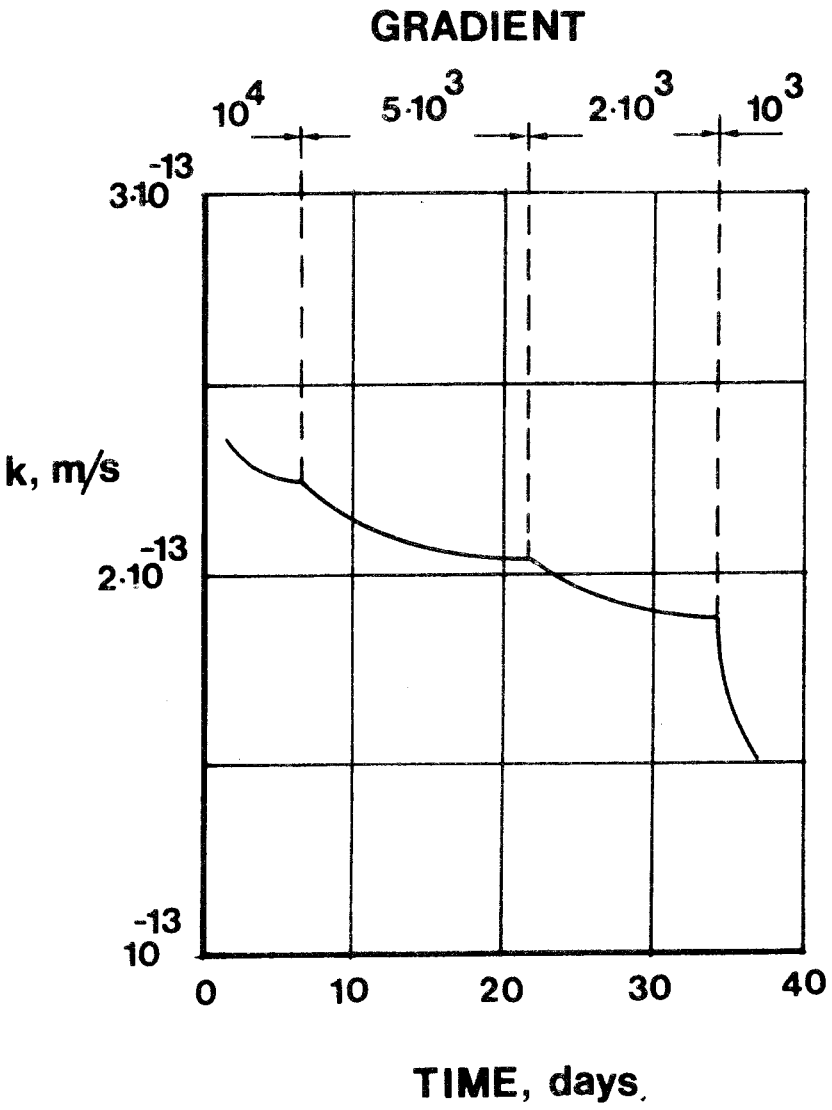

Fig. 6. Example of permeability test with smoothened curve for the coefficient of permeability k versus time after the test start.

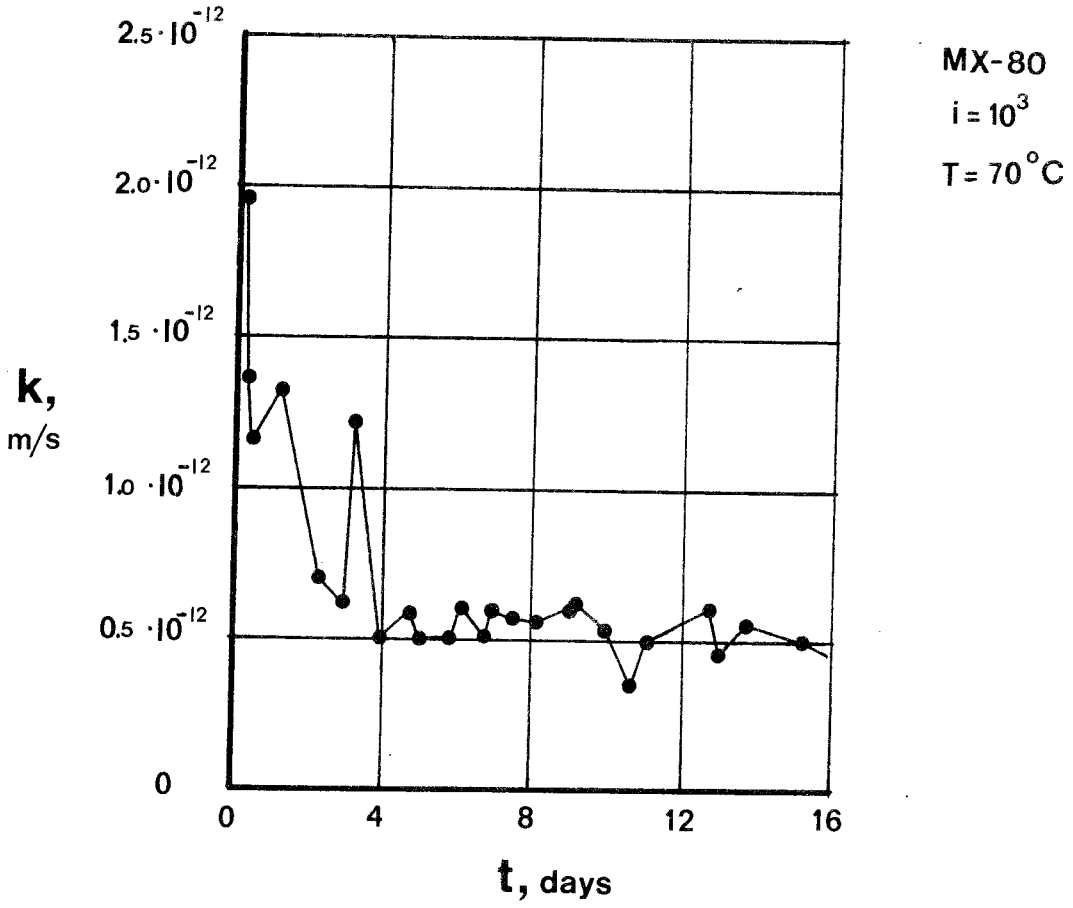

Fig. 7. Example of daily variations in permeability at a constant gradient. (Test 6, gradient = 10^3).

Table 2. The coefficient of permeability, k, evaluated from the percolation tests

Test No.	Material	Bulk density ρ_m, t/m^3	Temperature ^oC	Gradient	k m/s
1	MX-80	1.90	20	10^4	$2.2 \cdot 10^{-13}$
				$5 \cdot 10^3$	$2.0 \cdot 10^{-13}$
				$2 \cdot 10^3$	$1.9 \cdot 10^{-13}$
				10^3	$1.3 \cdot 10^{-13}$
2	MX-80	1.95	20	10^4	$2.3 \cdot 10^{-13}$
				$5 \cdot 10^3$	$2.0 \cdot 10^{-13}$
				$2 \cdot 10^3$	$1.9 \cdot 10^{-13}$
				10^3	$1.5 \cdot 10^{-13}$
3	MX-80	1.97	20	10^4	$1.2 \cdot 10^{-13}$
				$5 \cdot 10^3$	$1.0 \cdot 10^{-13}$
				$2 \cdot 10^3$	$9 \cdot 10^{-14}$
				10^3	$6 \cdot 10^{-14}$
4	MX-80	2.15	20	10^4	$2 \cdot 10^{-14}$
				$2 \cdot 10^3$	$2 \cdot 10^{-14}$
5	MX-80	1.93	70	$5 \cdot 10^3$	$3.8 \cdot 10^{-13}$
				$2 \cdot 10^3$	$3.6 \cdot 10^{-13}$
				10^3	$3.4 \cdot 10^{-13}$
6	MX-80	1.95	70	10^4	$7 \cdot 10^{-13}$
				$2 \cdot 10^3$	$6 \cdot 10^{-13}$
				10^3	$5 \cdot 10^{-13}$
7	MX-80	2.10	70	10^4	$1.8 \cdot 10^{-13}$
				$5 \cdot 10^3$	$1.8 \cdot 10^{-13}$
8	Erbslöh	1.94	20	10^4	$3.0 \cdot 10^{-13}$
				$5 \cdot 10^3$	$2.8 \cdot 10^{-13}$
				$2 \cdot 10^3$	$2.7 \cdot 10^{-13}$
				10^3	$2.7 \cdot 10^{-13}$
9	Erbslöh	2.21	20	10^4	$\sim 5 \cdot 10^{-14}$
				$2 \cdot 10^3$	$\sim 5 \cdot 10^{-14}$
10	Erbslöh	1.87	70	10^4	$3.1 \cdot 10^{-12}$
				$2 \cdot 10^3$	$3.1 \cdot 10^{-12}$
				10^3	$3.1 \cdot 10^{-12}$
11	Erbslöh	1.93	70	$5 \cdot 10^3$	$9.0 \cdot 10^{-13}$
				$2 \cdot 10^3$	$8.0 \cdot 10^{-13}$
				10^3	$7.0 \cdot 10^{-13}$
12	Erbslöh	2.13	70	10^4	$1.4 \cdot 10^{-13}$
				$5 \cdot 10^3$	$1.4 \cdot 10^{-13}$

The influence of the temperature increase from 20 to $70^{o}C$ is very obvious. At any particular density, the higher temperature increases the average permeability by a factor of approximately 3 to 7.

The theoretically predicted higher permeability of the Ca bentonite is experimentally evidenced.

DISCUSSION

General

The test results illustrate that pressure-induced water migration through saturated, highly compacted bentonite takes place at very low rates. The fact that the flow rate is gradient-sensitive and that the bulk density and temperature, as well as the type of adsorbed cation, largely determine the permeability is of great practical significance. The matters will therefore be discussed in some detail here.

Influence of the hydraulic gradient on the permeability

The redistribution of water and interparticle distances, i.e. the slow processes which lead to an improved homogeneity of aged, compact bentonite, may have produced a slight, successive reduction of the average width of the flow passages in the tests, and of the permeability as well. The observed permeability drop at decreasing hydraulic gradients may partly be caused by such microstructural rearrangement. Its influence must be minor, however, since it is known from preliminary investigations that the rate of ion migration through diffusion, which must also be strongly dependent on the width and continuity of the water passages, is not very much affected by a few

weeks of rest between the stage of water saturation and the start of the diffusion process. Furthermore, the permeability related to each hydraulic gradient in Fig. 6, actually approached a constant value. The deviations from DARCY's law are therefore true and require some relevant explanation, such as:

1. Electrokinetic coupling, e.g. the generation of an opposite osmotic flow when a liquid is forced through clay.

2. A heterogeneous microstructure of the aggregated type implies that a number of particles at the periphery of the aggregates are very weakly bound and therefore free to move even at very low flow rates of the pore water. Such particles may clog water passages thereby affecting the water flow.

3. A higher viscosity of mineral-adsorbed water than of surface-distant pore water implies that the movable fraction of the pore water is determined by the hydraulic gradient. Consequently, the evaluated permeability is also gradient-dependent.

The first effect can be assumed to yield a successive retardation of the flow. However, it is fairly unimportant compared with the other effects (OLSEN, 1961). The fact that the chemical pore water composition was the same at the saturation and at the percolation, is assumed to have minimized the set-up of electric potentials.

The second effect should be insignificant in the final state of microstructural homogeneity, at least at high bulk densities. At lower densities than the ones of interest in this

study, as well as in freshly compacted, dense, granulated bentonites, small particles may easily be transported through void passages by flowing pore water also at very low gradients. The influence of particle migration on pore water flow is two-fold. Firstly, particles will move irregularly through certain passages which temporarily become clogged, reopened and then clogged again, etc. This effect, which was noticed also by HANSBO (1960) in a similar study of illitic clay, produces a more or less irregular flow which may result in a variation in permeability of the kind illustrated by Fig. 7. Secondly, the net effect of a continuous water flow in one main direction is a successive clogging and an associated reduction of the permeability. Although both effects may be of some practical importance they can hardly be very significant in highly compacted bentonite since their high shear resistance certainly imply a very high degree of continuity of the particle network. They can, in fact, be explained by viscosity anomalies as shown in the subsequent text.

Influence of water viscosity anomalies on the permeability

Flow on a microscopic scale

Conventionally, flow on a microscopic scale in a porous medium is regarded as being governed by three equations; the equation of continuity, the equation of state, and the dynamical equation of motion (LAMB, 1932). It was early realized, however, that the difficulties involved in prescribing the nature of the flow channels and the interactions between the fluid and the porous media are such that the classical approach to solving flow problems is not useful. The major problem in describing, mathematically, water flow through highly compacted smectite-rich clays, is to define the flow character with special reference to the physical

state of the water. While water flow through clays of low density can be considered as the motion of a fluid with a definite and constant viscosity, it should rather be regarded as a shear-induced displacement of a "structured" medium in the case of dense bentonites. This is because the small interparticle distances imply that mineral-adsorbed water is largely involved in the flow process. In aged, homogeneous bentonite the largely constant interlamellar spacing is of the order of 5-15 Å for the bulk density interval 1.8-2.1 t/m^3. These spacings roughly correspond to 2 to 4 water molecule layers.[1)] In practice, the varying particle geometry and orientation yield a variation in void size as well (Fig. 8) and it is reasonable to believe that only larger interparticle and

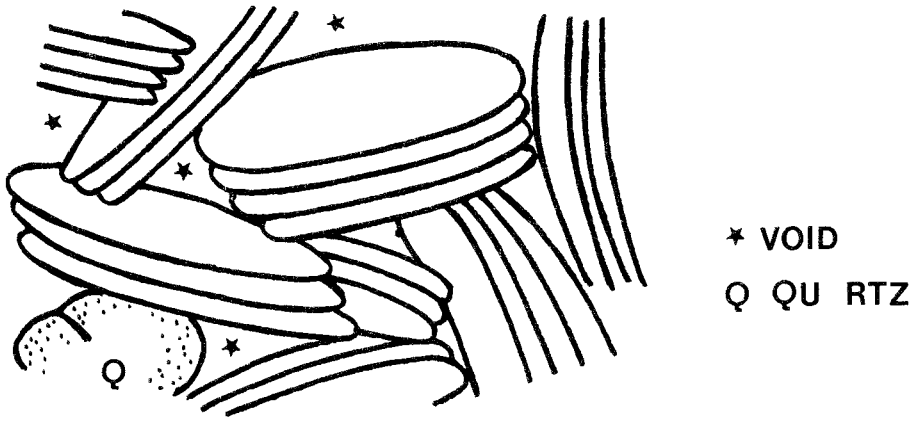

Fig. 8. Schematic picture of interparticle and interlamellar voids in dense bentonite.

and intraparticle voids let water through. Since the physical state of the pore water is essential in this respect it will be commented upon as an addendum to the discussion.

---

1) Actually, the coordination of water molecules at silica surfaces does not imply a simple correlation between the spacing and number of layers.

The mineral/water/electrolyte system

Energy is released in the course of the adsorption of the first 1-3 layers of water molecules onto surfaces of dry clay particles. This is partly due to the hydration of exchangeable cations but also of the surfaces of minerals. The exchangeable ions seem to hydrate without appreciable dissociation (LOW & MARGHEIM, 1979), and it is therefore reasonable to believe that the first few layers of molecules are firmly bound to clay minerals. Substantial evidence has in fact accumulated pointing to a very strong fixation of the first molecule layers and this affects interparticle and interlamellar (intraparticle) spacings. The author's current study of the swelling pressure of Na bentonites shows that maximum net repulsion and non-reversibility do not appear at the fairly large interparticle distances predicted by double-layer theories. In fact, they do not even appear at the very narrow distance 10 Å and this suggests that the swelling pressure is determined by the stability (strength) of interparticle water "lattices". 10 Å has been suggested as the approximate decay length for a presumably "steric" stabilizing water structure on phyllo-silicate surfaces by various investigators, such as DERJAGUIN & CHURAEV (1974), and ISRAELACHVILI & ADAMS (1978). Recent studies of proton relaxation of water adsorbed on silica glass surfaces (ALMAGOR & BELFORT, 1978) and experimental determination of the amount of nonfrozen water in frozen illitic clays (PUSCH, 1979) support the view that a few molecule layers are firmly adsorbed on most silica mineral surfaces.

The degree of structural order of such "vicinal" water does not necessarily have to be high, as DROST-HANSEN (1969) has pointed out. His water model consists of three zones with different structural and electrical properties (Fig. 9).

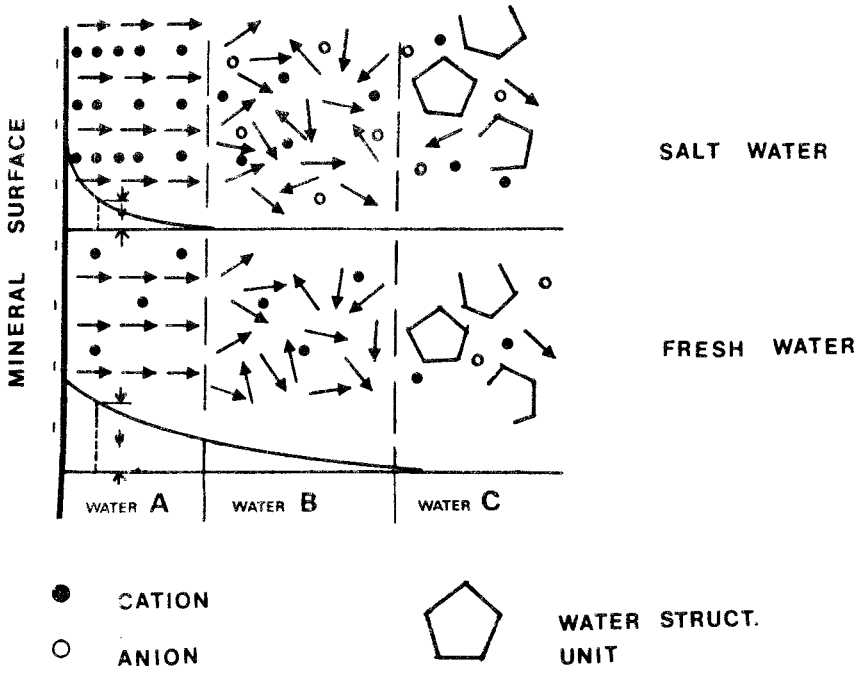

Fig. 9. Schematic picture of DROST-HANSEN's water model combined with electrical double-layers.

Zone A comprises densely spaced, "fixed" water molecules. The intermediate, B-zone, is characterized by a very low degree of ordering and by low viscosity; zone C consists of normally structured, "free" water.

Studies of the nuclear relaxation properties of water in illitic clays have disclosed short spin-spin coherence times which, in fact, suggests a high proton mobility and thus some degree of structural order (PUSCH, 1970). The results of the silica glass surface study by ALMAGOR & BELFORT" show that this order occurs in the vicinal water.

It can be concluded from these considerations that:

1. Interlamellar water films with a thickness of 5-10 Å are mechanically stable and inactive in water migration under the action of moderate hydraulic gradients. This means that, at high bulk densities, smectite particles consisting of packs of lamellae behave as non-permeable units. Water flow largely takes place where the interparticle or interlamellar distance exceeds about 10 Å, at least at low and moderate hydraulic gradients. At the highest gradients applied in the tests, certain interlamellar water molecule migration may possibly have taken place but it was then probably associated with displacements of adjacent lamellae.

2. The drop in structural stability of the water at increasing distance from an exposed mineral surface implies that water molecules are displaced close to the surface only at high shear stresses, while low stresses produce displacements at larger distances from the surface. This corresponds to a flow anomaly meaning that the permeability will increase at increasing hydraulic gradients. More water will simply be moved through increased shear stresses when the gradient is raised.

3. The displacement of water relative to a mineral surface is akin to the process of mutual displacement of mineral particles separated by thin water films. This points to the applicability of modern creep theory also to the present case.

Creep analogy

Recently, PUSCH & FELTHAM (1980) presented a creep theory valid for aggregated clay at moderate shear stresses, the main features of the theory being:

1. The clay is regarded as a heterogeneous system, comprising dense, strong structural elements (aggregates) connected by links of various strength, i.e. potential slip units (domains, cf. Fig. 10) with a dispersion of resistance to deformation.

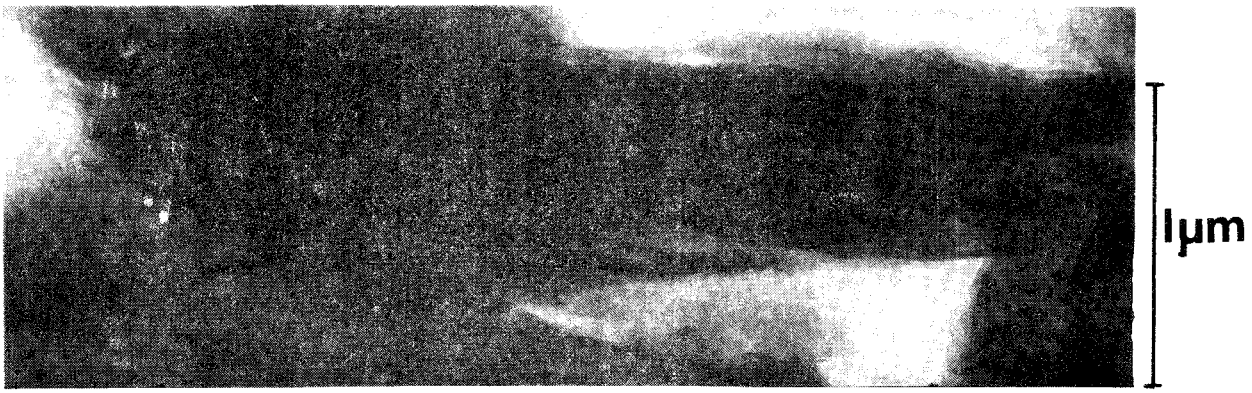

Fig. 10. Slip unit (domain) consisting of clay platelets with parallel basal planes separated by water films of different width.

2. The application of a shear stress produces a certain number of slip units. Their movements and the displacements and deformations of secondarily formed slip units make the main contribution to the overall observed strain. The slip, which has the character of activated atomic or molecular jumps, can be visualized as resulting in the form of shiftings of individual atoms or molecules as well as of patches of such units. The shiftings are considered as thermally assisted passages over energy barriers driven by the external stress.

3. The slip process leads to an interaction between bigger and stronger structural elements, which results in local stress relaxation and in an increase in the heights of the energy barriers for subsequent, activated jumps. It is thus a "hardening" process.

4. New links and particle bonds formed in course of the strain will also tend to strengthen the structure.

5. Regional redistribution of stresses, facilitated by slip, produces local stress concentrations. It will assist slip decreasing the heights of some energy barriers, and is thus a "softening" process.

It is quite obvious that a similar physical model can be applied to describe the movement of a structured fluid through a porous medium. The general features of a stochastic model which corresponds reasonably well to the physical prototype and which is relevant also in the present study are:

a. There is a spectrum of barrier heights for slip in the material (Fig. 11). The shape of the distribution curve reflects the microstructural heterogeneity and types of dominant bonds at different times after a stress change.

b. Each element of clay contains a certain number, n(u,t), of slip units in any given interval of the activation energy range.

c. In the course of slow strain the low energy barriers are triggered early, while higher ones are activated later. Also, new slip units are formed at the lower end of the energy spectrum.

d. The model allows both for slip which, when it takes place, takes a given slip unit up against a barrier by an amount either δu higher than the previous one, or lower by the same amount.

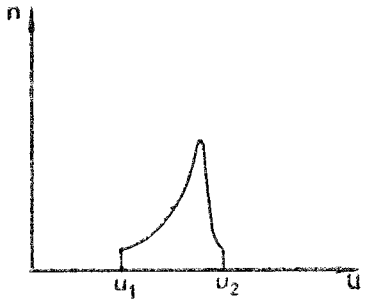

Fig. 11. Activation energy spectrum at a given time t after the onset of creep.

The derivation of a mathematical model for a particular case, which is also of interest in this context, has been outlined previously (PUSCH and FELTHAM, 1980), so only the basic steps are briefly recapitulated here.

At any given temperature only a limited energy spectrum $u_1 \leqslant u \leqslant u_2$ will be of significance in the determination of strain and strain rate. The number of potential slip units per unit volume held up at barriers of height u, is then $n(u,t)\ \delta u$ per energy unit, where t is time after the onset of creep, and δu one of the energy intervals into which we consider the spectrum between u_1 and u_2.

A basic assumption is that the attempt frequency of slip $\nu(u)$ is given by the ARRHENIUS rate equation:

$$\nu(u) = \nu_D \exp(-u/kT), \quad u_1 \leqslant u \leqslant u_2 \qquad (2)$$

where u is the barrier height. Here , ν_D is an atomic vibrational frequency of the order of 10^{12} per second. k is Boltzmann's constant and T the absolute temperature.

If slip has been activated at a certain point in the material, i.e. a barrier has been overcome, a contribution to the overall shear is made by the associated extension of the local slip-patch and the next barrier to be encountered by the same spreading slip-zone will be either higher or lower by an average amount δu. The magnitude of δu is determined by the amplitude of the internal stress field, and by the physical nature of the barriers.

It is reasonable to allow for an equal probability of slip following an activated jump of a patch, to occur so that the next barrier encountered by the patch is either higher or lower than the previous one, and considerations analogous to those familiar from the derivation of equations of diffusion then yield, on writing n for $n(u,t)$ for the continuity equation of the process:

$$\partial n/\partial t = D\, \partial^2 [n \exp(-u/kT)]/\partial u^2 \qquad (3)$$

$$D = \frac{1}{2} \nu_D (\delta u^2)$$

For low temperatures an appropriate solution of Eq. 3 is:

$$n(u,t) \propto p \cdot \exp(-p) \qquad (4)$$

with $p = \exp(u/kT)/\nu_D(t+t_o)$

where t_o is a "structure-sensitive" constant of integration which is usually practically zero for inorganic clays.

If the passage of a slip patch through the element of dimensions L (Fig. 12) displaces the part above the slip plane over the plane below by an amount b, then the resulting shear is b/L. If a slip unit does not traverse the whole element but advances only a certain distance on activation under the influence of the local stress field, then the shear strain will be:

$$\delta_\gamma = \left(\frac{b}{L}\right) \cdot \left(\frac{A^*}{L^2}\right) \qquad (5)$$

where A^* is the area swept over by the patch in jumping to the next barrier.

If slip has been activated at a certain point, the contribution to the overall shear is given by Eq. 5, so if there are n δu points per unit volume and unit of energy, where the barrier height is u, then in a cube of side L, the contribution δ_γ due to slip of all u-units is:

$$\delta\gamma_u = \left[n(u,t)L^3\right]\left(\frac{b}{L}\right) \cdot \frac{A^*}{L^2}\,\delta u \qquad (6)$$

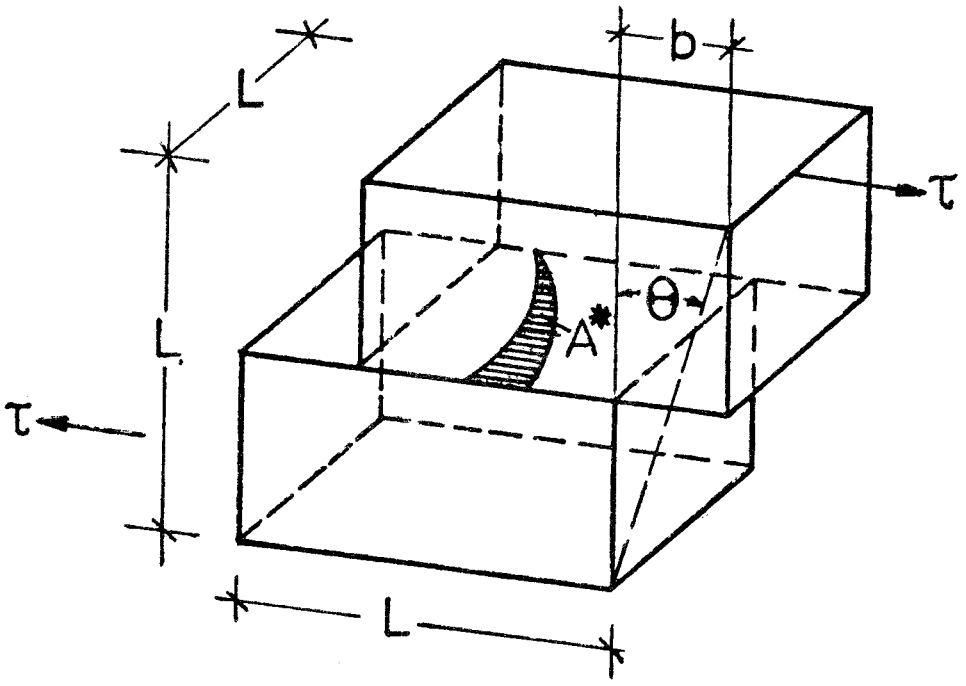

Fig. 12. Soil element with internal displacement produced by a slip. τ is the shear stress.

If the attempt frequency at all such points is $\nu_D e^{-u/kT}$, then the contribution by the u-interval to the strain rate is:

$$\delta\dot{\gamma} = \nu_D b A^* n(u,t)\ \exp\ (-u/kT)\,\delta u \qquad (7)$$

If each activated jump makes the same, average, contribution to the bulk shear strain of the specimen, the creep rate in shear will be:

$$\dot{\gamma} = b \cdot A^* \int_{u_1}^{u_2} e^{-u/kT} \cdot n(u,t)\,du \qquad (8)$$

On using Eq. (4) in Eq. (8) we obtain for $t_o = 0$:

$$\dot{\gamma} \propto \frac{1}{t} \qquad (9)$$

This is a commonly observed relationship for clays. An approximate estimate of the magnitude of the activation energies involved can be obtained by considering Eq. 2. A reasonable value of the jump rates $\nu(u)$ to lead to observable creep would be of the order of $1 s^{-1}$ which yields $u \sim 0.6$ eV. Such an activation energy indeed suggests that water is largerly involved in creep at ordinary temperatures and that the hardening mechanisms at least partly comprise water lattice re-formation.

In principle, Eq. 8 also describes the rate of movement of pore water through a heterogeneous clay particle network (or rather a large number of interconnected passages) provided that the movement of the fluid is entirely governed by the displacement of slip units held up at energy barriers of varying height. As in the creep analogy, the slip units consist of face-to-face grouped lamellae separated by water films of varying width. In narrow, permeable voids such units make up the larger part of the water mass, but wider passages certainly contain "free" water as well. The rate of flow following the application (or instant change) of a hydraulic gradient is therefore retarded as shown by Fig. 6, but a sufficient amount of free water normally flows through the system to yield, finally, a constant flow rate.

Three main conclusions can be drawn from the creep analogy:

I. The transient form of the flow/time relationship can at least partly be explained by the slip mechanisms involved in the stochastic model.

II. The "finite" jumps leading to temporary held-up of the slip units may well yield a "stick-slip"-type of flow on a macroscopic scale as is implied by Fig. 7.

III. If the movement of water through bentonite takes place according to the stochastic model, the influence of an increased temperature on the flow rate should be much stronger than predicted by the usual simple relationship between viscosity and temperature of free water.

The latter point deserves special attention and is dealt with separately in the subsequent text.

Influence of temperature on the permeability

Two essentially different relationships between temperature and permeability can be imagined; one representing a simple ARRHENIUS-dependence of the viscosity of liquids with a simple relaxation mechanism:

$$k_i \propto e^{-u/kT} \qquad (10)$$

where

k_i = coefficient of permeability
u = activation energy for flow
k = Boltzmann's constant
T = absolute temperature

and the other one derived from the basic equations of the stochastic creep model (cf. PUSCH & FELTHAM, 1980):

$$k_i \propto f(T)/t+t_o \qquad (11)$$

where

t = time after the onset of creep

t_o = constant of integration

$f(T)$ = temperature function, a simple assumption being $f(T) = T^n$ with n equal to or larger than 1.

We see that while Eq. 10 is based on the presupposition that time is not a determinant, Eq. 11 describes a retarded flow process, which thus agrees with the experiments. The latter equation should therefore be preferred but unfortunately the f(T) function has not been very well investigated. Creep experiments on various clays have shown that Eq. 11 applies very well with reference to the influence of time, and for a series of such tests on practically identical samples at different temperatures, the diagram in Fig. 13 was obtained. It indicates that the creep rate is increased by approximately 3 to 5 times when the temperature is raised from 20 to 70°C. This is in very good agreement with the observed permeability increase in the present study (cf. Table 2 and Fig. 16). Similar creep tests on bentonite need to be performed as well, and a test series is presently being planned.

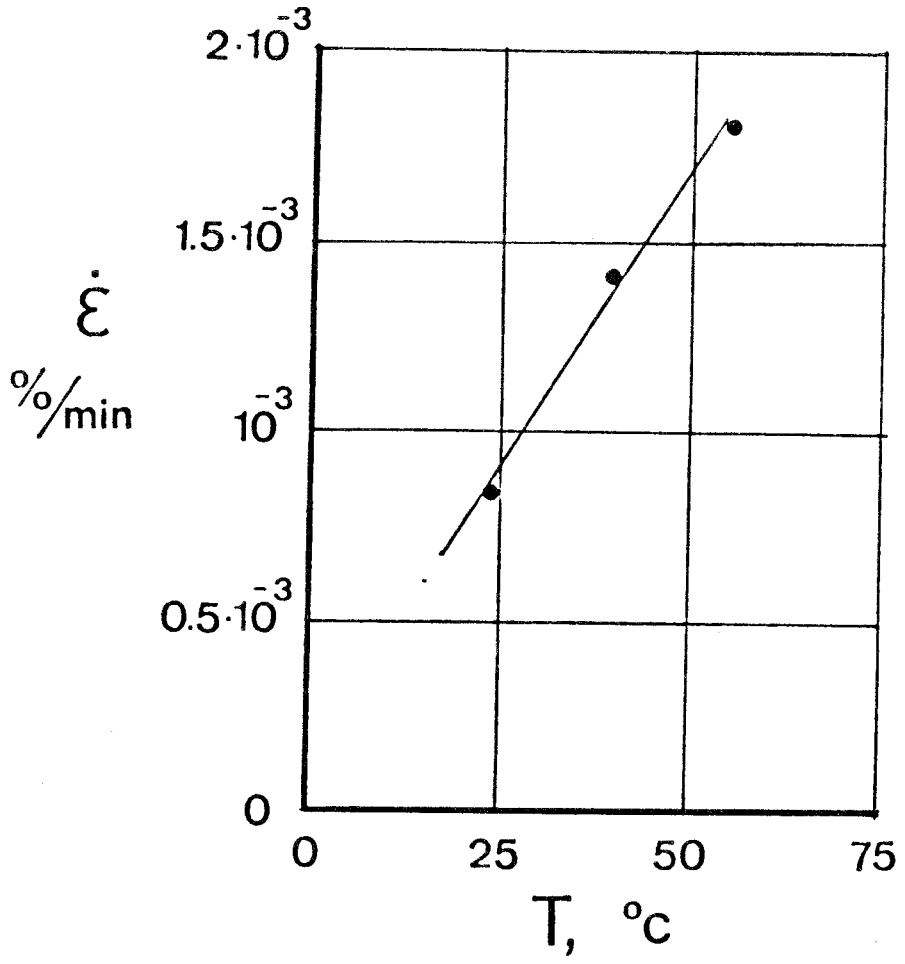

Fig. 13. Observed relationship between axial creep strain rate and temperature for t = 1 hour. Triaxial creep tests on illite; undrained conditions.

Influence of bulk density on the permeability

The strong impact of an increased density on the permability was obvious already at an early stage of this study. Thus, a literature survey of the permeability/density ratio of Na montmorillonite yielded the diagram in Fig. 14. The band accounts for variations in testing technique, hydraulic gradients, temperature, impurities etc.

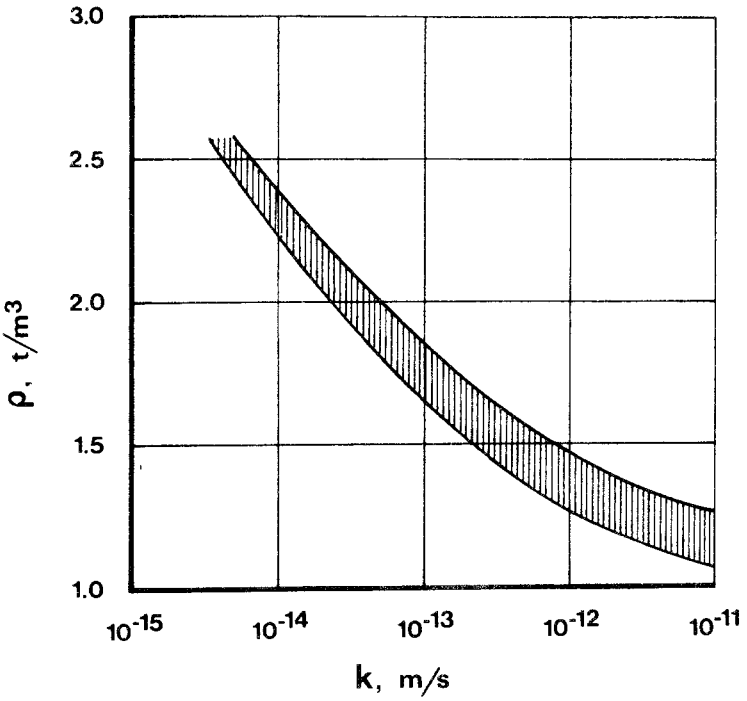

Fig. 14. Relationship between bulk density and the coefficient of permeability of Na montmorillonite according to a literature survey in early 1977.

The main reasons for the importance of the bulk density are implicitely given in the preceeding text. Thus, a largely increased bulk density means that the width of the water passages is very much reduced. Their continuity is thereby largely lost and, most important of all, the fraction of the pore water which is mineral-adsorbed and which shows viscosity anomalies is very much increased. To that comes an increased tortuosity, which is a measure of the actual flow path length in the system.

Tortuosity is conveniently expressed by the model in Fig. 15, which shows a soil consisting of equally spaced, anisometric particles arranged in a brick-like way. The angle, θ, between

the principal axes of the particles and the direction of permeation is assumed to correspond to the average degree of particle orientation. Starting from the DARCY and KOZENY/CARMAN equations, OLSEN (1961) derived a mathematical expression of the tortuosity, T, of flow which yields approximately twice as high T:s for n = 20 than for n = 80%, where n is the porosity. This ratio is representative of soil systems with the rather extreme anisometric particle shape which is characteristic of smectites. It suggests that tortuosity is a relatively important but not decisive flow-retarding factor at high bulk densities.

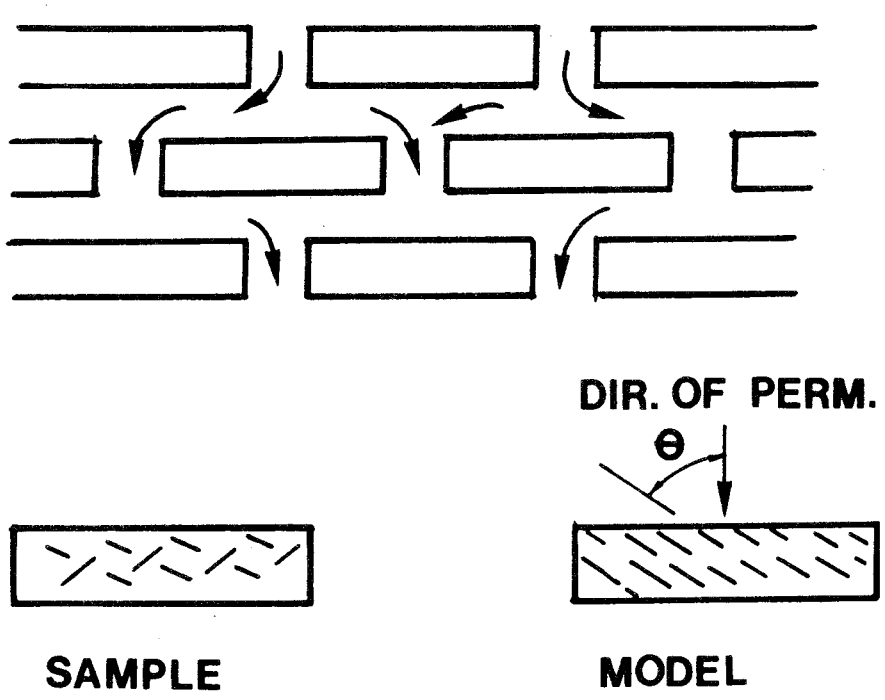

Fig. 15. OLSEN's physical model for derivation of a mathematical expression of tortuosity.

CONCLUSIONS, PRACTICAL IMPLICATIONS

The experimental part of the present study can be summarized by means of the two diagrams in Fig. 16 which show the coefficient of permeability as a function of the bulk density for the two investigated bentonites. It is obvious that high bulk densities reduce the permeability to very low values, but the Na bentonite experiments obviously did not yield as low values as the literature-derived ones, at least not at densities lower than 2 t/m^3. This may be explained by the fact that Wyoming bentonite is not a pure Na montmorillonite and that the present tests were made by using high hydraulic gradients.

The gradient-dependence is of utmost importance and at the low gradients which will finally be operative in a repository when the rock temperature is back to normal, the permability will most probably be of the order indicated by the literature survey for Na-bentonite (lower curve) or less than that (Table 3, first column). For Ca bentonite it seems reasonable to assume permeability values which are approximately 2 to 5 times higher. For the period when the temperature is of the order of 70°C in the bentonite, the permeability is estimated to be approximately 5-10 times higher than at 20°C for both clays. Since the hydraulic gradients are also higher in this period the most conservative values would then be those given in the second column of Table 3.

We can conclude from this that practically impervious conditions prevail when the gradients are low. Thus, with a regional gradient of 10^{-2} and a permeability of 10^{-13} m/s, the flow rate will not be higher than approximately 1 mm in 30 000 years.

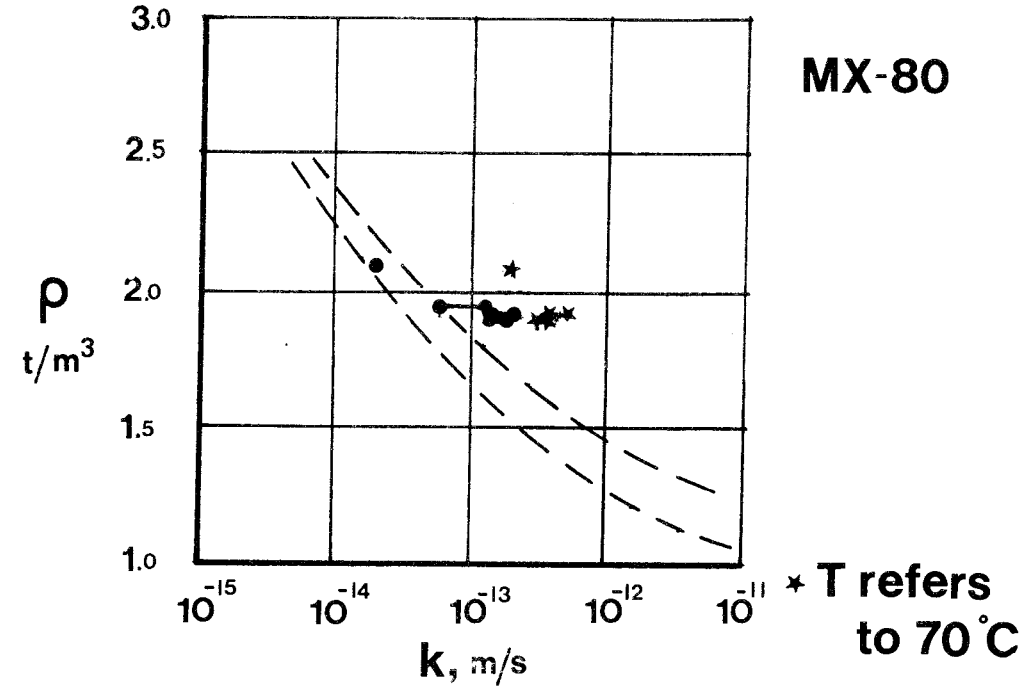

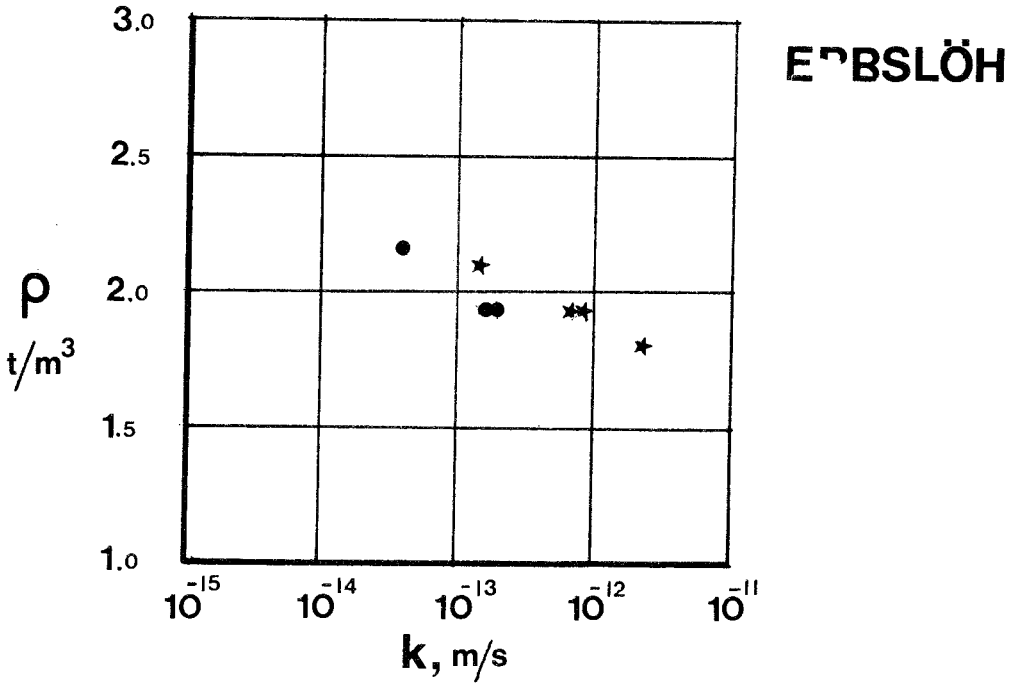

Fig. 16. The coefficient of permeability versus bulk density. Where two values are plotted for one and the same density, the left represents $i=10^3$, and the right 10^4. Broken curves are upper and lower boundaries of literature-derived values.

Table 3. Predicted permeability, k, m/s.

Bulk density ρ t/m^3	Final stage, low temperature, very low gradients		Early stage, 70°C temperature fairly high gradients	
	Na	Ca	Na	Ca
2.1	$1.5 \cdot 10^{-14}$	$8 \cdot 10^{-14}$	$1.5 \cdot 10^{-13}$	$2 \cdot 10^{-13}$
2.0	$2 \cdot 10^{-14}$	10^{-13}	$2 \cdot 10^{-13}$	$4 \cdot 10^{-13}$
1.9	$3 \cdot 10^{-14}$	$2 \cdot 10^{-13}$	$5 \cdot 10^{-13}$	$8 \cdot 10^{-13}$
1.8	$5 \cdot 10^{-14}$	$5 \cdot 10^{-13}$	$8 \cdot 10^{-13}$	10^{-12}
1.7	$8 \cdot 10^{-14}$	$8 \cdot 10^{-13}$	10^{-12}	$5 \cdot 10^{-12}$

REFERENCES

ALMAGOR, E. & BELFORT, G., 1978. Relaxation studies of adsorbed water on porous glass. Journal of Colloid and Interface Science, Vol. 66, No. 1.

DERJAGUIN, R.W., & CHURAEV, N.V., 1974. Structural component of disjoining pressure. Journal of Colloid and Interface Science, Vol. 48, pp. 249-255.

DROST-HANSEN, W., 1969. Water near solid interfaces. Industrial and Engineering Chemistry. Vol. 6., pp. 2048-2056.

HANSBO, S., 1960. Consolidation of clay, with special reference to influence of vertical sand drains. Swed. Geot. Inst., Proc. No. 18, (pp. 27-61).

ISRAELACHVILI, J.N., & ADAMS, G.E., 1978. Measurement of forces between two mica surfaces in aqueous electrolyte solutions in the range 0-100 nm. Journal of Chemistry, Society Faraday Transactions, I, Vol. 74, pp. 975-1001.

LAMB, H., 1932. Hydrodynamics. 6th Ed. Cambridge University Press, London.

LOW, PH. F., & MARGHEIM, J.F., 1979. The swelling of clay: I. Basic concepts and empirical equations. Soil science of America Journal, Vol. 43, No. 2, May-June, pp. 473-481.

OLSEN, H.W., 1961. Hydraulic flow through saturated clays. Thesis submitted in partial fulfillment of the requirements for the degree of Doctor of Science in Civil Engineering, MIT.

PUSCH, R., 1970. Clay microstructure. Document D:8, National Swedish Building Research Council, Stockholm.

PUSCH, R., 1979. Unfrozen water as a function of clay microstructure. H.L. Jessberger ed. Ground Freezing, Developments in Geotechnical Engineering, Vol. 26, Elsevier Sci. Publ. Co., Amsterdam.

PUSCH, R., 1980. Water uptake migration, and swelling characteristics of unsaturated and saturated highly compacted bentonite. SKBF/KBS Teknisk Rapport 80-11.

PUSCH, R., & FELTHAM, P., 1980. A stochastic model of the creep of soils. Géotechnique, December issue 1980.

TERZAGHI, K., 1923. Die Berechnung der Durchlässigkeitsziffer des Tons aus dem Verlauf der hydrodynamischen Spannungserscheinungen. Akademie der Wissenschaften im Wien. Sitz. ber. Mathematisch - natur - wissenshaftl. Klasse-IIa. 132, (pp. 125-138).

FÖRTECKNING ÖVER KBS TEKNISKA RAPPORTER

1977-78

TR 121 KBS Technical Reports 1 - 120.
Summaries. Stockholm, May 1979.

1979

TR 79-28 The KBS Annual Report 1979.
KBS Technical Reports 79-01--79-27.
Summaries. Stockholm, March 1980.

1980

TR 80-01 Komplettering och sammanfattning av geohydrologiska undersökningar inom sternöområdet, Karlshamn
Lennart Ekman
Bengt Gentzschein
Sveriges geologiska undersökning, mars 1980

TR 80-02 Modelling of rock mass deformation for radioactive waste repositories in hard rock
Ove Stephansson
Per Jonasson
Department of Rock Mechanics
University of Luleå

Tommy Groth
Department of Soil and Rock Mechanics
Royal Institute of Technology, Stockholm
1980-01-29

TR 80-03 GETOUT - a one-dimensional model for groundwater transport of radionuclide decay chains
Bertil Grundfelt
Mark Elert
Kemakta konsult AB, January 1980

TR 80-04 Helium retention
Summary of reports and memoranda
Gunnar Berggren
Studsvik Energiteknik AB, 1980-02-14

TR 80-05 On the description of the properties of fractured rock using the concept of a porous medium
John Stokes
Royal Institute of Technology, Stockholm
1980-05-09

TR 80-06 Alternativa ingjutningstekniker för radioaktiva jonbytarmassor och avfallslösningar
Claes Thegerström
Studsvik Energiteknik AB, 1980-01-29

TR 80-07 A calculation of the radioactivity induced in PWR cluster control rods with the origen and casmo codes
Kim Ekberg
Studsvik Energiteknik AB, 1980-03-12

TR 80-08 Groundwater dating by means of isotopes
A brief review of methods for dating old groundwater by means of isotopes
A computing model for carbon - 14 ages in groundwater
Barbro Johansson
Naturgeografiska Institutionen
Uppsala Universitet, August 1980

TR 80-09 The Bergshamra earthquake sequence of December 23, 1979
Ota Kulhánek, Norris John, Klaus Meyer, Torild van Eck and Rutger Wahlström
Seismological Section, Uppsala University
Uppsala, Sweden, August 1980

TR 80-10 Kompletterande permeabilitetsmätningar i finnsjö-området
Leif Carlsson, Bengt Gentzschein, Gunnar Gidlund, Kenth Hansson, Torbjörn Svenson, Ulf Thoregren
Sveriges geologiska undersökning, Uppsala, maj 1980

TR 80-11 Water uptake, migration and swelling characteristics of unsaturated and saturated, highly compacted bentonite
Roland Pusch
Luleå 1980-09-20
Division Soil Mechanics, University of Luleå

TR 80-12 Drilling holes in rock for final storage of spent nuclear fuel
Gunnar Nord
Stiftelsen Svensk Detonikforskning, september 1980

TR 80-13 Swelling pressure of highly compacted bentonite
Roland Pusch
Division Soil Mechanics, University of Luleå
Luleå 1980-08-20

TR-80-14 Properties and long-term behaviour of bitumen and radioactive waste-bitumen mixtures
Hubert Eschrich
Eurochemic, Mol, October 1980

TR 80-15 Aluminium oxide as an encapsulation material for unreprocessed nuclear fuel waste - evaluation from the viewpoint of corrosion
Final Report 1980-03-19
Swedish Corrosion Institute and its reference group

TR 80-16 Permeability of highly compacted bentonite
Roland Pusch
Division Soil Mechanics, University of Luleå
1980-12-23

TR 80-17 Input description for BIOPATH
Jan-Erik Marklund
Ulla Bergström
Ove Edlund
Studsvik Energiteknik AB, 1980-01-21

TR 80-18 Införande av tidsberoende koefficientmatriser i BIOPATH
Jan-Erik Marklund
Studsvik Energiteknik AB, januari 1980

TR 80-19 Hydrothermal conditions around a radioactive waste repository
Part 1 A mathematical model for the flow of groundwater and heat in fractured rock
Part 2 Numerical solutions
Roger Thunvik
Royal Institute of Technology, Stockholm, Sweden
Carol Braester
Israel Institute of Technology, Haifa, Israel
December 1980

TR 80-20 BEGAFIP. Programvård, utveckling och benchmarkberäkningar
Göran Olsson
Stanley Svensson
Studsvik Energiteknik AB, 1980-10-14

TR 80-21 Kartläggning av tekniker och metoder för ytkarakterisering av glas/keramer
Bengt Kasemo
Mellerud, augusti 1980

TR 80-22 Evaluation of five glasses and a glass-ceramic for solidification of Swedish nuclear waste
Larry L Hench
Ladawan Urwongse
Ceramics Division
Department of Materials Science and Engineering
University of Florida, Gainesville, Florida
1980-08-16